EUDET-Memo-2010-15

Validation of GEANT4 hadronic models using CALICE data

John Apostolakis and Andrea Dotti[*],
Erika Garutti[†],
Alexander Kaplan[‡],
Mikhail Kosov[§] Vladimir Uzhinskiy[¶],
David Ward[‖],
on behalf of the CALICE collaboration

February 18, 2011

[*] CERN, Geneva, Switzerland
[†] DESY, Hamburg, Germany
[‡] University of Heidelberg, Heidelberg, Germany
[§]
[¶] CERN & JIRN
[‖] University of Cambridge, Cambridge, United Kingdom

1 Introduction

This paper is an overview of five years of work performed within the EUDET framework, on validation of simulations. This part of the EUDET task focused on improving and extending the modelling of hadronic showers in fine-grained calorimeters.
A description is given of the major improvements to key physics models, in particular the Geant4 FTF Fritiof model and the CHIPS model.
During these studies the need to eliminate the use of the approximate parameterised LEP models, was confirmed; work on FTF concentrated on improving its modeling for interactions important at lower energies. The CHIPS model has been significantly improved and new cross-sections were provided for pion, kaon and hyperon interactions; a preliminary version of these extensions of the CHIPS model was available in the development releases of 2010, and a first validation is now possible.
Extensive comparisons of further hadron data from the Calice collaboration with the most recent GEANT4 physics lists are presented. New observables are reported, including energy profiles after the identified interaction point. Additional observables separate the response into different sections of the calorimeter: in the first few layers after the interaction; in the next vicinity (where gammas would interact) and in distant layers. Overall reasonable agreement is seen; however deficiencies in energy deposition in the layers near the interaction and in the subsequent rise were clearly observed. These have provided feedback for further improvement of the models.
An overview of the CALICE GEANT4 validation studies is presented.

2 Geant4 modeling of hadronic interactions

The main models for hadronic interaction in Geant4 are the high-energy string models (QGS and FTF) for energies typically above $5-10$ GeV, and the cascade models (Bertini and Binary) for intermediate energies. To treat the excited nuclei from higher energy collisions, and also collisions below about $200MeV$, a family of de-excitation models is available: this includes an initial stage with a precompound model and then the competition between evaporation processes and potentially fission or Fermi breakup.
The alternative CHIPS model has been used for stopping particles, electronuclear and gamma-nuclear interactions. A recent extension to CHIPS enables it to model hadronic interactions for all hadrons. (The CHIPS package also includes treatment of elastic scattering of neutrons and of the quasi-elastic scattering of nucleons and pions.)

The Geant4 Quark Gluon String (QGS) model implements a version of the QGS model due to N. Amelin[1] and N. Kolmogorov. It is used to describe the interactions of nucleons, pions and kaons at energies above 10-15 GeV.

The QGS model requires a model for the de-excitation of nuclei after the initial interaction. The first model used for this purpose was the Geant4 Pre-Compound model, which include evaporation and fission. The Geant4 QGS model together with the Pre-compound de-excitation describe thin-target data well at about 15 GeV, but not below 10 GeV.

A key set of models which have been used for simulating below about 15 GeV has been the parameterised model. These were part of the first hadronic physics models available in Geant4, and were derived from GHEISHA[2]. Fixes and some improvements in these parameterised GHEISHA models were introduced to create the Low Energy Parameterised (LEP) and High Energy Parameterised (HEP) models.

These models do not attempt to conserve energy in each interaction, but instead were targetted for describing average energy deposition in calorimeters. The details of interactions were approximated, and sampling was done from parameterisation using simple models of the outgoing particles. As a result it is not possible to obtain accurate differential quantities, or correlations from these models. Only very approximate estimates of resolutions are thus possible.

A key strength of these models is that they are applicable for all meson and hadron projectiles and all targets. For this reason they have been utilised to simulate all interactions of hyperons in all physics lists up to Geant4 9.3. A key weakness is that interactions below 10 GeV show significant deviation from conservation of the average energy, with the sum of the energy outgoing from an interaction ranging from $10 - 25\%$ below the incident total energy.

At low energy (below few GeV) the most promising models for interaction are the cascade models. These treat the interaction of projectiles with target nucleus as a series of independent, incoherent collisions. Only the original particles or the products of a collision may interact. Nuclei are modeled either as a set of discrete nucleons or as shells with given densities. Two cascade models in Geant4 have been used for application in HEP to date: the Bertini-type and Binary cascade models[3].

The Geant4 Bertini-type cascade is based on a re-engineering of the INUCL cascade code and includes the Bertini intra-nuclear cascade model with excitons, and a dedicated set of de-excitation models, including a pre-equilibrium model, a nucleus explosion model, a fission model, and an evaporation model. A nucleus is modelled as a set of spherical shells of constant density, and the results of discrete hadron-nucleon interactions are sampled from a set of multi-

particle final states. Intermediate energy nuclear reactions from 100 MeV to 5 GeV are treated for protons, neutrons, pions, photons and nuclear isotopes.
The Bertini cascade model can be used for proton, neutron, pion and kaon primaries and has been extended for interactions up to 10 GeV. Recent improvements corrected the internal modeling of the hadron-hadron interaction, extending it to produce additional multi-particle final states, in particular those with 6 or more particles. The Bertini model implementation is not able to simulate the rescattering of secondary hadrons produced by the high energy models (e.g. QGS) inside the nucleus.
An alternative to the Bertini cascade model is the Binary Cascade (BIC). The Geant4 Binary Cascade is an intranuclear cascade propagating primary and secondary particles in a nucleus. Each nucleus is modelled as a set of discrete nucleons, positioned at sample locations. Only binary interactions are modelled, using the production, interaction and decay of resonances. Cross section data are used to select collisions. Where available, experimental cross sections are used by the simulation. Propagating of particles is the nuclear field is done by solving the equation of motion numerically. The cascade terminates when the average and maximum energy of secondaries are below set thresholds. The remaining fragment is treated by the Geant4 precompound and de-excitation models. BIC model, followed by Precompound and de-excitation, can be used also for the rescattering (inside the nucleus) of secondaries particles produced by the Quark- Gluon-String model. This is utilised in just a few physics lists, including the QGS_BIC physics list.

2.1 Combining models into "Physics List" configurations.

Models of hadronic inelastic interactions are applicable (and reliable) over a limited range of projectile energies for inelastic interactions. Only the CHIPS model/module can cover the full energy range, using a single model that amalgamates smoothly its original decay model and a string interaction model.
To cover the full energy range, a combination of hadronic models is required. A combination attempts to utilise each model in its best, 'strict' validity range and typically extending these in energy in order to cover the remaining, intervening energies. As a result the full set of physics interactions, including EM and hadronic interactions, are assembled into Geant4 physics lists: these apportion the range of projectile particle types and energies between the physics processes and models.
Only the LEP and HEP models are utilized (exclusively) in the LHEP physics list. The overlap between low energy LEP and high energy HEP models stretching from 25-55 GeV.

This combination is used in the QGSP physics list, for all interactions above 25 GeV for pions and nucleons. Each interaction between 12 and 25 GeV may occur using either the LEP or QGS model: the model used is sampled randomly with a probability which depends linearly on energy and become 1 for the LEP model at 12 GeV and 1 for the QGS at 25 GeV.
In the QGSP physics list, other particles are modeled using the parameterised LEP and HEP models.
The models were also utilised in all Geant4 physics lists for hyperons and anti-nucleons up to and including in release 9.3. The only exception is in 9.3, since when the CHIPS physics list uses CHIPS models for both hyperons and anti-nucleons.
The introduction of CHIPS-based modeling for hyperons (and anti-nucleons) in Geant4 release 9.3 (December 2009) enables the creation of physics lists which do not use parameterised models, including FTFP_BERT and QGSP_FTFP_BERT.
QGSP_BERT_CHIPS retains LEP only for the nucleons, pions and kaons, in particular to bridge the energy interval between Bertini and QGSP (between $10 - 25$ GeV).
The LEP and HEP models have significant shortcomings: energy is not conserved in the interaction, spectra do not agree with recent data (since 1985) and the partition of energy between pions and nucleons disagrees with expectation. In the recent year comparisons with LHC test-beam data have shown that the LHEP physics list poorly describes the response of calorimeters to impinging hadrons, compared with physics lists based on string models (QGS, FTF).
For this reason the need to identify models to replace the use of LEP and HEP was recognised, in particular for nucleons and pions.

3 The challenges for the simulation of hadron interactions

No models are applicable from few MeV up to TeV region required for HEP applications. The available models have limitations, including energy range of applicability. Significant gaps exist between the regions where models are clearly applicable: for example the assumptions of most string models best interactions above 20-30 GeV, whereas most cascade models' assumptions break down above 1-3 GeV.
In the past years the detailed comparison with LHC test-beam data has allowed to improve the simulation code substantially and, at the same time, to identify the areas where additional work is needed. For LHC experiments the first

priority is the description of the response to hadrons in calorimeters. The theory based models (QGS, FTF physics lists) have proved to be the best model to describe experimental data.
Shower shape play also a key role for some aspects of the data analysis (cluster reconstruction, jet corrections based on weighting techniques), however the granularity of LHC calorimeter allows only for a partial comparison of the details of shower dimensions.
After the improvement of the hadronic shower shape (see below), a few key challenges emerged:

- The description of the hadronic shower shape, longitudinal and lateral - for pions and protons, to a level better than 20% at 10 lambda.

- The description of the energy response of calorimeters in the region of $10 - 25$ GeV, where a non-physical dip in response was present - blamed on the transition between hadronic models and the use of parametrized models.

4 Improvement of modeling

Two of the most important additions have been made in physics modeling during the past decade were the addition of intranuclear cascade for lower-energy projectiles (nucleons, pions and sometimes kaons below 3-5 GeV) and the creation of a separate channel for quasi-elastic interactions in the high energies string models.
A separate quasi-elastic channel was added to the Geant4 Quark Gluon String (QGS) and FTF model was undertaken since Geant4 release 8.3 (May 2007.) Accounting for 5-10% of the non-elastic cross-section, the new modeling of these interactions allowed a significant improvement of the hadronic shower shape.
The biggest revisions in Geant4 hadronic modeling during the past three years have been made in the CHIPS, FTF, Bertini and pre-compound models.
The Bertini cascade was upgraded using improved cross-section for pion-nucleon interactions, and the correction of multi-particle meson-nucleon final states.
A review and improvement of the pre-compound and de-excitation models of Geant4 was also carried out[4].
In the following two important improvements to the description of hadronic interactions relevant for present and future colliders are described in detail.
The new CHIPS event generator model allows for a coherent treatment of hadronic interactions at all energies and for all projectile in a novel theoretical framework. This characteristics makes this model the main candidate

to solve the problem of the transition region and provides a replacement for parametrized models for kaons, anti-nucleons and hyperons projectile.
The FTF (Fritiof) high energy string model is based on diffraction description of the hadronic interactions. In this sense has the possibility to improve the description of longitudinal shower shapes (making them longer) especially for protons. Recent important improvements (in particular the introduction of Reggeon cascading) allows for an extension to lower energies of the model. It is thus possible to construct a physics list that does not require parametrized models in the intermediate energy-region.

4.1 Implementation of the Fritiof model in Geant4

To address the challenge of obtaining accurate modeling of hadronic inelastic interactions in the energy region between 5 and 10 GeV, the choice was made to focus on extending the string models down in energy. The goals were to improve the agreement with new measurements at intermediate energies (4-12 GeV), and to obtain sufficient predictive power for physics quantities which have not been measured. An important constraint was the need to do this without degrading the good description of physical observables at the end energies (at 3 GeV in Bertini and at 15 GeV in QGS and FTF). We sought also a smooth transition for all physical quantities (observable or not), without unphysical steps or inflections.
The high energy models implemented in the GEANT4 covered different energy ranges the Quark-Gluon String model (QGS) working above 12 GeV and and the Fritiof model (FTF) [5, 6] starting around 5-7 GeV. Before the recent upgrades, both models did not include either a description of formation time in the collision or a mechanism for creating s-channel resonances in binary reactions and for the destruction of the nucleus. These deficiency made it hard to extend them to lower energies, in particular below 5 GeV. As a result, physics lists for HEP applications relied instead on cascades and even the LEP parameterised models. For example, in the QGSP_BERT physics list the Bertini cascade model is relied upon up to nearly 10 GeV; above this the LEP parameterised model is used, and phased out with a model overlap range from 12 to 25 GeV. Even in the FTFP_BERT physics list the overlap between BERTini and FTF spanned the range from 6 to 8 GeV, due to the
The need to extend one of the string models down to $3-4$ GeV was to offer improved modeling, which avoided the deficiencies of the Bertini cascade above $3-4$ GeV. Definiciencies identified include an apparent excess "output" energy in nucleons, and the need to approximate multi-particle final states (due to the lack nucleon-nucleon collisions which result in 6 or more products.)

It is expected that the concept of the formation time concept is required in order to obtain a smooth transition from high to low energy domains.

The formation time ansatz was not yet implemented in the QGS and FTF string models. This ansazt forbids reinteraction of the particles which result from a collision for a given time; this can be interpreted as time that allows them to "form" or stabilise. It is possible to couple this with the option to reinteract lower energy products inside the target nucleus using the binary cascade BIC model.
All products with energy below a certain threshold, typically of a few GeV, could be tracked if this option is used - as in the QGS_BIC physics list. (The Bertini model in Geant4 (BERT), although used more widely, can not be used for technical reasons, including the need to track time.)
Due to the lack of a formation time additional low energy evaporated and pre-equilibrium particles are created in many interactions. This reflected on local energy deposition and shower profile, properties critical for detector design.
The path chosen for improvement was to extend a Geant4 high energy model to lower energies. This would reduce the energy range for which the cascade models. The Fritiof model was chosen as the most promising experimental test bed, due to its simpler structure compared with the QGS model.

The Fritiof model treats all hadron-hadron interactions as binary reactions. Each of the resulting hardons can be in the ground state or in an excited state. So, three types of interactions can be distinguished: $h_1 + h_2 \rightarrow h_1 + h_2'$, $h_1 + h_2 \rightarrow h_1' + h_2$, or $h_1 + h_2 \rightarrow h_1' + h_2'$. The interaction of two hadrons, h_1 and h_2, typically produces two hadrons in excited states, h_1' and h_2', such as $h_1 + h_2 \rightarrow h_1' + h_2'$. The model assumes that the excited hadrons have a continuous spectrum of masses. This is called a "non-diffractive interaction". Alternatively, if one of the hadrons is in the ground state $(h_1 + h_2 \rightarrow h_1 + h_2')$ the reaction is called "single diffraction dissociation".
The excited hadrons are considered as QCD-strings, and the LUND string fragmentation model[7, 8] is applied to simulate their decays. The model implemented in Geant4 takes into account other reactions, of the type $h_1 + h_2 \rightarrow h_3 + h_4$, as well as the elastic scattering. Separate weights for hN elastic scattering, hN diffractive and non-difractive interactions have been introduced and tuned.

Several model refinements have been introduced also to improve the behavior of the model for lower energy projectiles, those below $5 - 10$ GeV. Phase-space restrictions have been introduced for the fragmentation of the low mass strings which are created in the diffractive interactions. In addition "kinky strings" were implemented. These include additional transverse momentum in the generation of the strings, a feature included in the original model[6]. As a result, the description of the transverse momentum distributions of produced particles has been improved.

Low energy pion-nucleon and nucleon-nucleon interactions proceed mainly through s-channel Δ-resonance formation, including $\pi+N \rightarrow \Delta$, and $N+N \rightarrow \Delta + N$. In the reggeon field theory approach these processes are treated as quark exchanges between colliding hadrons. A direct quark exchange was introduced in the model. According to the reggeon theory, the cross section of the processes decreases with energy increase as $1/s^{0.5-2}$.
The probability of a quark exchange was written as

$$W_{q.exc.} \sim A\ e^{-B\cdot(y_{pr}-y_{tr})}, \tag{1}$$

where y_{pr} and y_{tr} are projectile and target rapidities, and A and B are parameters that were tuned. The following reactions were considered and described: $\pi^- + p \rightarrow n\pi^0$, $\pi^- + p \rightarrow n2\pi^0$, $\pi^- + p \rightarrow n\pi^+\pi^-$, $\pi^- + p \rightarrow p\pi^+\pi^0$, $\pi^- + p \rightarrow p\pi^+2\pi^-$, $p + p \rightarrow pn\pi^+$, $p + p \rightarrow pp\pi^0$ and so on. The corresponding experimental data for the tuning were taken from the CERN-HERA compilation [9].
The FTF/Fritiof model assumes that in the course of a hadron-nucleus interaction the string (originating from a projectile) can interact with intra-nuclear nucleons and become highly excited. The probability of the multiple interactions is calculated in the simplest approximation. A cascading of secondary particles is neglected as a rule. Due to these simplifications, the original Fritiof model did not describe nuclear destruction and slow particle spectra.
In the past, within Geant4, the Fritiof model was either

- coupled directly to the Pre-compound model (which was given the name FTFP), or
- used the Binary cascade to rescatter slow products (named FTF_BIC), before the Binary model used the Precompound model for de-excitation.

A number of limitations and deficiencies were identified in these approaches. In particular the Binary cascade model has an important limitation: it cannot model accurately the interactions of pions above about 1.5 GeV (which corresponds to the highest measured resonance which is relevant.) For these reasons an improved approach was sought. As a result the model has been coupled to a specialized, simplified, cascade.
The standard approach of particle cascades in nuclei and the concept of the formation time were criticized by reggeon theory experts: the approaches do

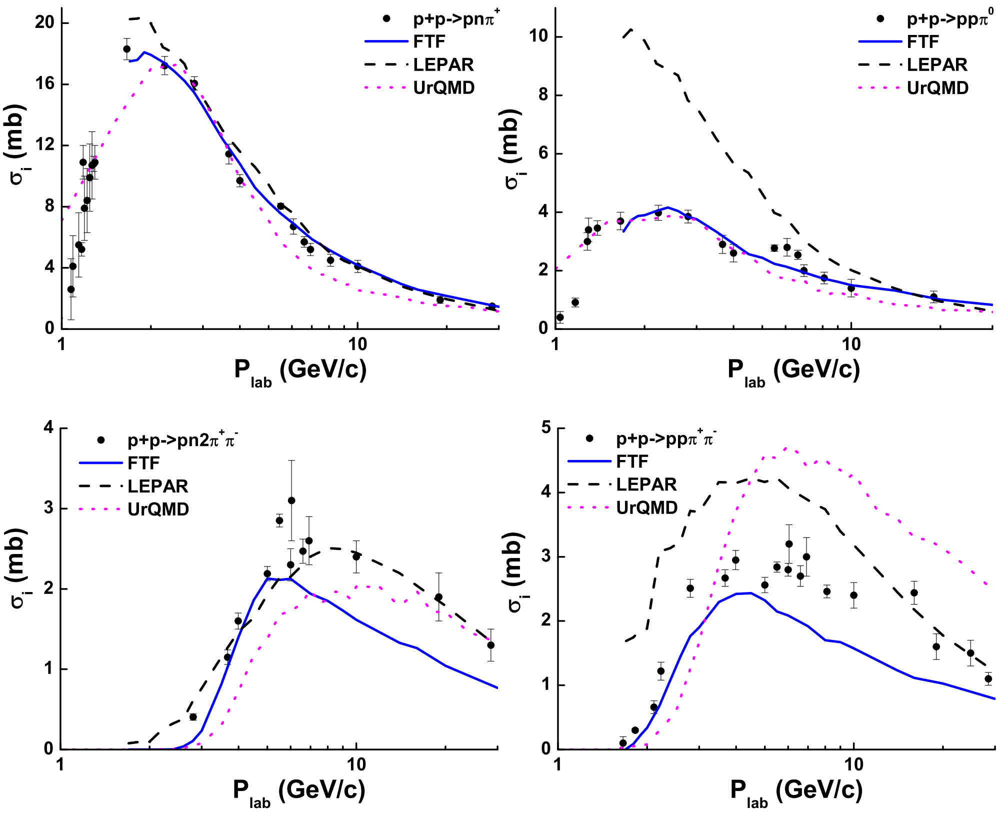

Figure 1: Cross sections of $pp-$interactions. Points are data from CERN-HERA compilation[9]. Solid lines are results of the improved FTF model. Dashed lines are results of the low energy parameterized model (LEPAR) of GEANT4, which was based on the GHEISHA package used by GEANT3. Dotted lines represent the UrQMD model [10, 11] results.

not consider the space-time structure of strong interactions. It was proposed that cascading could be correctly treated in the reggeon theory by considering of the so-called enhanced diagrams. An attempt to take them into account was presented in Refs. [12], where a simplified model was proposed.
This cascade model is now implemented and coupled to the GEANT4 FTF model. It gives a possibility to simulate nuclear destruction in the first, fast stage of interactions and then it passes the remnants to the pre-compound and pre-equilibrium module. The momenta due to Fermi motion of the nucleons involved in the reggeon cascading are sampled using an algorithm proposed in Ref. [13]. The parameters were taken from Refs. [13, 14] and further tuned.
High energy models do not have, as a rule, an algorithm for the calculation of the residual excitation energy. We attempted to resolve this by coupling this model with a cascade model. Various alternative possibilities have been considered, as those discussed by Pshenichnov[15]. The simplest recipe is to ascribe each wounded nucleus and each nucleon involved in the cascading a constant value of the excitation energy. This is implemented in the interface between the FTF model and GEANT4 pre-compound model. The value has been tuned for the FTF model, while ensuring the conservation of energy and momentum. The result of the HARP experiment served as reference data for the tuning of parameters. In particular the results of the analysis of the HARD-CDP group on proton production[16, 17, 18] in hadron-nucleus interactions at $P_{lab} \sim 3 - 15$ GeV/c were used. A satisfactory description of these data has been reached.
In summary, the FTF/Fritiof model of Geant4 has been substantially improved. A transition to a Reggeon cascade mode and a restriction using phase space for the s-channel final states at low energies were introduced. All these enabled the revised model to describe the hadron-nucleon and hadron-nucleus interactions starting from $P_{lab} =$ 3 GeV/c and to achieve a smooth transition with the Bertini cascade. In addition the energy dependence of physical quantities across the challenging energy region of $5 - 15$ GeV is much improved, correcting the steps observed in the QGSP_BERT physics list. For future work, the Reggeon cascade and s-channel reactions (which were added to the FTF model) hold promise for use with QGS, the other high energy string model.

4.2 Implementation of CHIPS physics package in Geant4

The CHIPS code is a quark-level event generator for the fragmentation of hadronic systems into hadrons. It is based on the Chiral Invariant Phase Space (ChIPS) model [2, 3, 4] which employs a 3D quark-level $SU(3)$ approach.

The phase space refers to the phase space of massless partons. As a result only light (u, d, s) quarks are considered.
A new CHIPS model for nuclear reactions, applicable at all energies, was implemented in Geant4 during the period February 2009-January 2010. Using it over the full energy range (for one or more incident particle) avoids transitions between different separate Geant4 models, which are suitable for restricted energy ranges.
Instead it blends a new inelastic model with the existing comprehensive CHIPS de-excitation model, and the older, restricted low-energy interaction. The new inelastic CHIPS model is similar to the well known Kaidalov's Quark-Gluon String (QGS) model with an additional "string-at-rest" 3D object named a Quasmon.
The CHIPS 1D string has a number of differences:

1. Projectiles and targets are split up in partons according to the CHIPS phase space algorithm instead of the parameterized QGS $x\alpha(1-x)\beta$ randomization

2. CHIPS partons are massles ($M_p = 0$), where p stands for quarks (Q), diquarks (DQ), anti-quarks (aQ), or anti-diquarks (aDQ)); by contrast they are massive in the QGS model

Consequently, there is no low limit for the string mass ($M_{string} >> M_{parton}$) and for the projectile energy. Yet if a string mass is smaller than the sum of masses of two minimal hadrons, then the string itself can not hadronize. For example this is the case for the string with no baryon number or strangeness ($B = S = 0$), if it is below the mass of two pions.
To address this case and hadronize the low mass strings there is an additional CHIPS algorithm:

1. If there are hadrons (H) from hadronization of other strings, the low mass string (S) can be converted to a hadron (the $H + S \rightarrow H + H$ reaction)

2. Two strings can be fused into one string if their ends can annihilate ($Q+aQ$, $DQ+aDQ$) or both ends can be converted to partons ($Q+Q \rightarrow DQ$, $DQ + aQ \rightarrow Q$, $aQ + aQ \rightarrow aDQ$, $aDQ + Q \rightarrow aQ$)

3. After the fusions, the trial loop continues ($H+S => H+H$, new fusions etc.) until all strings are hadronized

4. If the two-strings-fusion is impossible, all low mass strings are fused together in a single 'emergency' Quasmon; this is subsequently given over to 3D hadronization

At low energies string fusion is problematic. To avoid this direct Quasmons are created. The nucleus absorbs energy proportional to the path length traversed as the projectile crosses it:

1. A parameter $\kappa \simeq 1.5$ GeV/fermi is used to govern this

2. The nucleus thickness for impact parameter b is $L(b) = T(b)/r(0)$

3. The string energy absorbed by the nucleus is $E_L(b) = \kappa \dot{L}(b)$

4. If $E < E_L(b)$, the direct Quasmon is created without the string fusion

5. If $E > E_L(b)$, the string fusion algorithm produces hadrons; the hadrons with the lowest rapidity are re-absorbed until they have a total energy $E_L(b)$ and used to create a Quasmon in the nucleus

6. A problem remains in the Geant4 implementation: if the string fusion ends up with an emergency Quasmon (case d. above), the lowest rapidity hadrons are not added to the Quasmon, so the nuclear fragmentation is underestimated

The CHIPS algorithm as implemented includes a nuclear scaling effect, to limit reinteractions and thus reduced the number of outgoing particles. At high energies $E >> E_L(0)$ the differential multiplicities (invariant spectra divided by inelastic cross-sections) are energy independent for each particular nucleus. The dependence on the target nucleus scales as $A^{1/3}$.
The original CHIPS model was tested at low energies (pion capture, anti-proton annihilation) and for special reactions (photo- and lepto-nuclear reactions). The new CHIPS model was tested recently for proton incident (pA) interactions at 90 MeV.
Additional testing and tuning are necessary at high energies. The main part of the algorithm to be tuned is the competition between the quark fusion hadronization (a string like hadronization in vacuum) and the quark exchange hadronization (knocking out of nuclear fragments by the excited Quasmon).
The CHIPS algorithm can be applied to all SU(3) hadrons, photons, leptons (splitting of virtual photons to quark-antiquark pairs) and neutrinos (splitting of virtual Z or W bosons to quark-antiquark pairs). Currently heavy c, b, and t quarks are not implemented.
All hadronic processes (other than inelastic ion-ion interactions) were implemented in the Geant4 CHIPS Physics package.

1. Stopping of all negative hadrons and $\mu-$-mesons (in all Geant4 physics lists).

2. Elastic scattering of all hadrons (the relative differential pA spectra are temporary used for all hA elastic reactions) and ions. Thanks to the EUDET support, the CHIPS elastic cross-sections for all hadrons at all energies were implemented to Geant4.

3. Inelastic reactions at all energies for all particles - using the new extended CHIPS model

4. A CHIPS model is used for photo and lepto-nuclear interactions at all energies in the CHIPS physics list. (Note that in other physics lists the CHIPS photo- and lepto-nuclear processes utilised only up to 3 GeV. Above this a QGS model is used)

5. A new CHIPS alternative for the neutron HP package was created. The elastic low energy CHIPS neutron cross-sections were improved and extended to cover 300 isotopes. Systematics for the non-elastic = (n,γ) + inelastic (including fission) CHIPS cross-sections for 300 isotopes have been prepared. The implementation has not yet been completed. At present low energy neutrons in the CHIPS physics list are converted into photons at about 1 MeV. As a result the calorimeter response is overestimated

6. As at high energies the synchrotron radiation is important not only for electrons and positrons (the standard Geant4 implementation), the faster CHIPS synchrotron radiation algorithm for all particles was implemented. Other CHIPS Physics package electromagnetic (EM) processes have not been implemented. Instead the Standard Geant4 EM set of processes was used

4.3 Additional modeling improvements

Improvements have also been undertaken in other hadronic models. Both the Bertini cascade model and the Precompound/Evaporation module are utilised by the production Geant4 physics lists for HEP, including the established QGSP_BERT and its emerging alternative FTFP_BERT.
A major overhaul of the pre-compound model and all the channels of de-excitation was carried out during the past three years [4]. All components of the pre-compound models were reviewed, including the condition for transitioning to the de-excitation phase. In the dexcitation phase, there was an overhaul of all channels and their associated components. Major improvements were undertaken in the fission. The evaporation model was refined, and the implementation of the Generalised Evaporation Model improved. This enabled

the creation of a hybrid of these, which allows the creation of large nuclei by direct evaporation, while retaining the description of light nuclei (up to alpha) of the original model. With the contribution of the original authors, the multi-fragmentation model was revised to reflect fully the original model description. A more detailed description of this work is beyond the scope of this report.

5 Expectations and open issues

A number of characteristics of the different modeling choices is apparent from the comparison of the products of reactions. We compare the sum of energy of outgoing particles. For nucleons we utilise the kinetic energy and for other particles their total energies (with this choice we investigate the energy available in the interactions).
The "invisible" or "lost" energy is defined as the imbalance between projectile energy (kinetic energy for nucleons and total energy for mesons) and the sum of the corresponding energies of the products. This unbalance is thus the energy lost in nuclear break-up. From energy conservation of the reaction $h+T \rightarrow X$ where T is the target nucleus and h is the incoming hadron (meson or nucleon):

$$\begin{aligned}
E_h + Z_T m_p &+ (A_T - Z_T)m_n + Q_T = \sum E_{out} \\
E_h + Z_T m_p &+ (A_T - Z_T)m_n + Q_T = \\
& \sum_{nucleons} E^{kin}_{out} + N_p m_p + N_n m_n + \\
&+ \sum_{fragments} (E^{kin}_{out} + Z_{out} m_p + (A_{out} - Z_{out})m_n + Q_{out}) \\
&+ \sum_{mesons} E_{out}
\end{aligned}$$

Where Z_i and A_i are the number of protons and number of nucleons of the nucleus i and Q_i is its binding energy. N_p and N_n are the number of free protons and neutrons in the final state. The second sum extends over all nuclear fragments in the final state. Since the totatal number of protons and neutrons is conserved in the hadronic interaction, the equation simplifies to:

$$E^{meas}_h - \sum_{nucleons,fragments} E^{kin}_{out} + \sum_{mesons} E_{out} = \sum_{fragments} Q_{out} - Q_T \qquad (2)$$

E^{meas}, the "measurable" energy, corresponds to E^{kin} for protons, neutrons and to E^{tot} for pions. This relation can be extended to include anti-nucleons with $E^{meas} = E^{tot} + m$ (to take into account that if anti-nucleons are created a corresponding nucleon is also created or if a anti-nucleon projectile is absorbed

it can annihilate with a nucleon from the target nucleus).
In general, this relation is only approximated, since different models provide different descriptions of this "invisible" energy (in the case of parametrized models this relation does not hold, since there is no guaranteed energy conservation)[1]. In particular the QGS model leads to the least energy lost, whereas the FTF and Bertini models have the most energy lost.
The energy fraction in different outgoing particles is also monitored. For the test case of a negative pion projectile on a Fe target using Geant4 release 9.3 patch 1, a number of potential issues have been identified:

- an excess of energy in the form of protons and neutrons is produced by the Bertini cascade in the range $5 - 10$ GeV;
- lower production of π^0 by Bertini at low energies (10% energy fraction at 1 GeV to 17% at 5GeV, and underestimation by FTF compared to other models(substantially revised in Geant4 9.4 towards agreement).
- the ratio of π^0 to charged pions is reduced by a move from Bertini or LEP to FTF(P)
- a higher fraction of energy into charged pions by LEP than QGSP, then FTFP and least Bertini for $E > 6$ GeV. This can be seen in figure2.
- a lack of strange particle production at energies from $5 - 20$ GeV by all models, with the exception of CHIPS.

5.1 Summary of results from LHC test-beams and simplified calorimeter setups

During the test-beam campaigns of the LHC Experiments, ATLAS, CMS and LHCb experiments used Geant4 to simulate the detectors that were put in the beam-line.
Stringent requirements were set on the simulation of the LHC setups [19]. Focus was put on the simulation of hadronics interactions and hadron showers in calorimeters. Three observable were studied in details:

- response: measured energy in the calorimeters as a function of beam energy. It is usually obtained from a gaussian fit of the measured energy distribution

[1] Theory driven models (QGS, FTF, BERT) should always conserve energy, however it has been shown that there are infrequent but significant deviations. Currently a review of these models is undergoing to ensure strict adherance to the conservation laws.

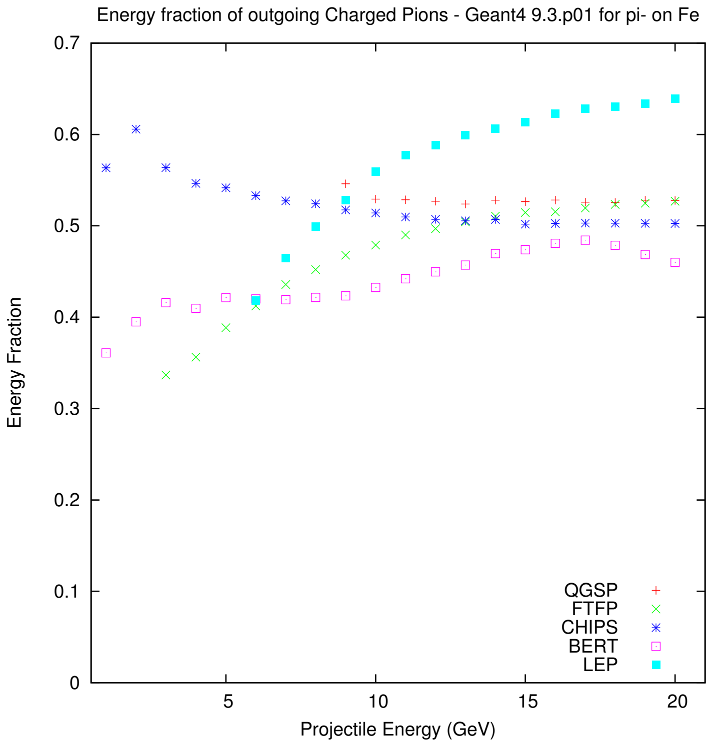

Figure 2: The ratio of the total energy of outgoing pions versus the total energy of the incoming pi^- projectile for a iron target.

- resolution: defined as the standard deviation divided the mean of the measured energy distribution. Both parameters are obtained from a gaussian fit
- partial lateral and longitudinal shower profiles: mean energy measured in the different compartments in which the calorimeters are segmented.

In most cases a limited set of physics lists was compared, chosen to feature models which have existed for an extended period; some new models were included, to address As a result the comparisons typically spanned the QGSP, QGSP_BERT physics lists, and sometimes the older lists LHEP which included only parameterised models and its variant LHEP_BERT which introduced the Bertini cascade. The new, improved FTF model was not available in time for many comparisons. The detailed comparisons of the shower developments in the calorimeters [20, 21] have shown that the QGSP_BERT physics list is the one that better describes test-beam data for ATLAS and CMS setups. LHCb, having less stringent requirements on calorimeters, adopted the LHEP physics list in production.

6 Results from LHC experiments

6.1 Response

The physics list QGSP_BERT is the closest to the pion test-beam data. The agreement is within $2 - 3$ %, with QGSP_BERT response higher than in the data [22, 23]. The beam energies available in the LHC test-beams were either below 9 GeV, or above 20 GeV.
Based on the findings of LHC experiments, starting from Geant4 version 9.3 (released in December 2009) some significant improvements have been achieved:

- The Fritiof model has been retuned (using thin-target data), improved (with the inclusion of quark-exchange) and extended to lower energies (by coupling to a Reggeon cascade). FTFP_BERT physics list provides now a response very close to QGSP_BERT and a smooth behaviour as a function of the beam energy.
- The new physics list CHIPS shows a smooth response as a function of the beam energy, as expected due to the absence of a rigid transition thresholds between its string and fragmentation components. In the first, experimental version of CHIPS, the response is too high, but tuning with

thin-target data is still ongoing and improvements are expected in the next versions.

For the response of protons, the agreement between simulation and test-beam data is more or less at the same level as for pions, although protons have been tested less extensively.

6.2 Energy resolution

The physics list QGSP_BERT describes the calorimeter energy resolution for pions within $\sim$ 10% [22, 23]. The energy resolution is typically narrower in the simulation than in data.
Similar energy resolutions are produced in Geant4 version 9.3 by the following physics lists: FTFP_BERT, QGSP_FTFP_BERT and FTFP_BERT_TRV. The experimental physics list CHIPS produces a too narrow energy resolution, but tuning with thin-target data is in progress.
For the energy resolution of protons, the agreement between simulation and test-beam data is more or less at the same level as for pions, although protons have been tested less extensively.

6.3 Longitudinal shower profile

The QGSP_BERT physics list produces pion longitudinal shower profiles that are shorter than data by $\leq$ 10% up to about 10 λ (the typical thickness of hadron calorimeters).
Proton longitudinal shower profiles are significantly shorter than observed in test-beam data: $\sim$ 30% up to about 10 λ [24].
For the physics lists of interest in Geant4 version 9.3 the longitudinal shower profiles are described as follows:

- QGSP_FTFP_BERT is very similar to QGSP_BERT for both pion and proton showers. This shows that replacing LEP with FTF does not affect the longitudinal shower profile in the energy range of the LHC testbeam setups.

- FTFP_BERT and FTFP_BERT_TRV physics lists have very similar longitudinal profiles, for both pion and proton showers, in good agreement with data, within about $\pm$ 10 % up to about 10 λ. This shows that changing the transition region between FTF and BERT has negligible effect on longitudinal shower profiles in the energy range of the LHC testbeam setups.

- CHIPS physics list produces longitudinal profiles longer than data by $\sim$ 20 % up to about 10 λ, for both pion and proton showers.

6.4 Lateral shower profile

There is only one LHC calorimeter test-beam result for the lateral profiles of pion and proton showers: the ratio of the energy measured in the bottom and central modules of the ATLAS TileCal set-up with beam sent at 90°. Based on it, we can draw the following conclusions for the energy range of LHC testbeam setups.
The physics list QGSP_BERT produces pion and proton lateral shower profiles that are narrower than data by $\sim$ 15 % [24].
In Geant4 version 9.3, CHIPS physics list describes very well the lateral profiles of both pion and proton showers. QGSP_FTFP_BERT is very close to QGSP_BERT; similarly for FTFP_BERT in the case of pion showers, whereas it is closer to data in the case of proton showers.

6.5 Transition between models

The CMS experiment has found that the calorimeter energy response in its HCAL test-beam setup, as a function of the pion beam energy, presents an unphysical discontinuity around 9-10 GeV. The ATLAS experiment confirmed the same problem for its calorimeter test-beam setups.
The origins of this discontinuity have been studied in detail in the past two years. It is now clear that the effect is caused by the use of the parametrized models for particle interactions in the energy range $9.5 < E_{kin} < 25$ GeV [25].
As a strategy to reduce the dependence on the parametrized models and to address the issue we have studied the performance of the FTFP_BERT Physics List, which has a reduced dependence on the parametrized models and it has different transition regions; and the CHIPS one, that does not depend at all on these parametrization and does not have, by construction, any strong transition.
We have performed simulations of a $10\lambda_I$ depth and wide sampling calorimeter (100 periods made of a 16.8 mm thick iron slab followed by 4 mm thick slab of scintillator). Impinging pions of different kinetic energies (from 1 to 500 GeV) have been simulated.
From our studies we have shown [26] that the FTFP_BERT and CHIPS do not show this problem in any of the usual calorimetric observables (response, resolution, shower shapes). LHC experiments are thus considering the possibility to use a Fritiof based physics list as the production ones in the near future.

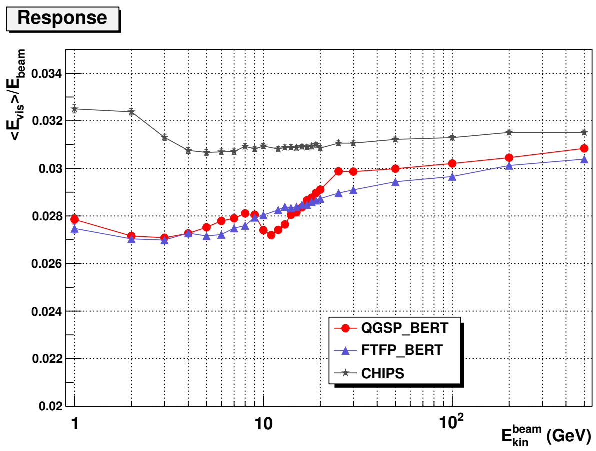

Figure 3: Simulated response in a simplified scintillator/iron sampling calorimeter for negatively charged pions as a function of primary kinetic energy. Different Geant4 Physics Lists are shown for comparison. Statistical and systematic errors are also shown, in many cases they are smaller than the symbol size. Development version geant4-09-03-patch-02 (September 2010) has been used to produce data.

7 The CALICE prototype calorimeters

The CALICE collaboration has been performing research and development on calorimeters intended for precision measurements at a future lepton collider. Prototypes of electromagnetic and hadronic calorimeters optimised for the Particle Flow approach have been built aiming for a jet energy resolution of 3-4% at the International Linear Collider [27, 28, 29]. As well as testing the hardware concepts, the CALICE data are able to test simulation models of particle showers in unprecedented detail owing to the highly granular readout of the calorimeters.

In this paper we report on some of the data taken in 2007 in the CERN H6 test beam. The layout of the CALICE calorimeters and the beam instrumentation are discussed in [30, 31].

The three calorimeters used were:

- A Si-W ECAL [32] using 30 layers of tungsten sheets wrapped in carbon fibre as absorber, and silicon wafers segmented into a 6×6 array of diode pads as active detectors. Each diode had a size of 1×1 cm^2.
- An analogue HCAL [31] using iron as absorber and 38 layers of scintillator tiles with analogue readout as the active medium. The tile size was 3×3 cm in the shower core. The thickness of the iron sheets was 18 mm.
- A tail catcher and muon tracker (TCMT) which was also an iron calorimeter with 16 layers of 5 cm wide scintillator strips. The thickness of the iron sheets was 20 mm for the first eight layers, and 100 mm in the rear section.

The ECAL and HCAL were mounted on a movable stage, providing the possibility to translate and rotate the calorimeters with respect to the beam. The extremely high granularity of the CALICE prototype allows three dimensional pictures of hadronic showers to be acquired. An impression of the granularity is provided by the following numbers. One ECAL cell is about 1×1 Molière radii (R_M) in size and the average longitudinal segmentation is 1 radiation length (X_0) or 0.03 interaction lengths (λ_{int}). In the AHCAL one cell has a size of about 0.85×0.85 R_M and a longitudinal segmentation of 1 X_0 or 0.15 λ_{int}. This granularity can be exploited to determine precise shower properties (e.g. the position of the first hadronic interaction, energy density, shower shape) and hence to validate different physics aspects implemented in Monte Carlo models.
Figure 4 shows the schematic setup at the SPS H6 test beam area. Positive and/or negative pion showers in the energy range 8-80 GeV have been investigated. The response of all the calorimeter cells in the individual detectors is equalised and calibrated using broad muon beams provided at the test beam site which provide an approximation to minimum ionising particles (MIP). The response of the AHCAL cells is corrected for the SiPM non-linearity. More details on the performance of the ECAL are found in [32] and about the AHCAL can be found in [33].
A detailed model of the detectors and of the beam instrumentation has been implemented in Mokka version 7.02 [34]. Mokka is a Geant4-based application able to simulate full ILC detector geometries as well as the CALICE setup. For all the studies presented the response in the simulated detectors is digitised so as to come as close as possible to data.
Unless otherwise specified version 9.3 of Geant4 was used for all physics lists except for CHIPS, for which the patched version 4.9.3.p01 was used.

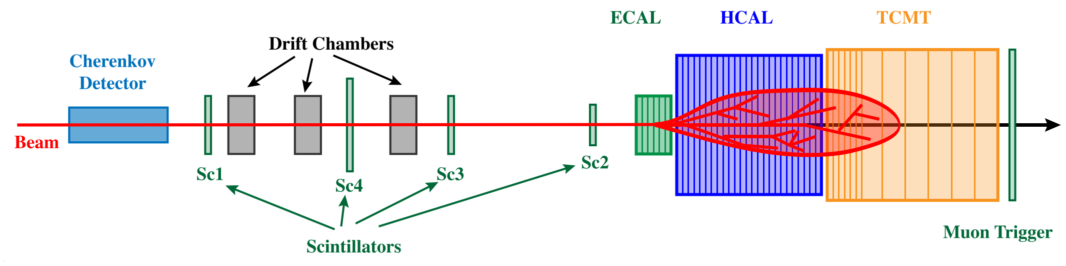

Figure 4: Schematic view of the CALICE experimental setup at CERN. Shown are the three CALICE calorimeters tested during this period: the electromagnetic calorimeter (ECAL), the hadronic calorimeter (AHCAL) and tail catcher and muon tracker (TCMT).

8 Validation of models using AHCAL data

Various observables are used to compare different aspects of simulation to data, from the fully integral energy deposited in the calorimeter to the differential variables like shower profiles and shower moments. Details on the calibration of the AHCAL and the validation of the Monte Carlo (MC) digitisation are given in [33].

8.1 Total visible energy

The ratio between the reconstructed energy for simulated and real negative pion showers is shown in figure 5 at beam energies of 8 to 80 GeV. The CHIPS physics list shows an energy independent overestimation of roughly 8%, while the response of the other physics lists varies with energy. The overestimation in CHIPS could be expected, since the low energy neutron cross-sections are not yet properly implemented in this model [35]. The other physics lists all tend to slightly underestimate the response at the lower energies, show a gradual rise with respect to the data as energy increases, and overestimate the response by $\sim$4-7% at 50-80 GeV.

8.2 First hard interaction and track segments

The high granularity of the CALICE AHCAL provides the capability for topological reconstruction within a shower. The first hard interaction can be located accurately, and in addition track segments from secondary hadrons produced within the hadron showers can be identified using a simple tracking algorithm.

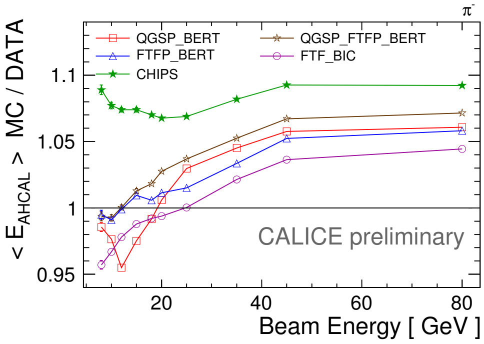

Figure 5: Ratio between the reconstructed energy in the AHCAL from simulation and from data for negative pion showers as a function of beam energy. All physics lists except CHIPS show an energy dependent behaviour.

The accuracy of the algorithm used to determine the position of the first hard interaction was studied by comparing with the true MC information about the end-point of the incident pion. In about 74% of the cases the error in the position determination is within ±1 calorimeter layer (≈ 3 cm).
From the distribution of the position of the first hard interaction as a function of the calorimeter depth one can directly extract the effective nuclear interaction length of pions in the material mix of the AHCAL, for data and MC. This is a consistency check of the validity of the algorithm and it yields the same effective nuclear interaction length, $\lambda_{int} \sim 30$ cm for all those physics lists which using the same pion cross section. The exceptions are LHEP which has a larger cross-section and a $\lambda_{int} \sim 26$ cm, and CHIPS which has a smaller cross-section and a $\lambda_{int} \sim 31$ cm). Data is found to be consistent with the majority of the models yielding a value of $\lambda_{int} \sim 29 \pm 1$ cm.
The algorithm used to find tracks created by minimum ionising particles in the cascade relies on identifying isolated hits and works on a layer-by-layer basis. The algorithm intrinsically limits the angle of reconstructed tracks to $\theta_{3\times3} < 58°$ for tracks in the $3 \times 3\text{cm}^2$ tiles (the corresponding limits for the larger tiles are $\theta_{6\times6} < 72°$ and $\theta_{12\times12} < 81°$). The fake track rate of the algorithm is at a negligible level of few per mil.
Figure 6 shows a typical hadronic shower in the AHCAL. Here, minimum ionising track segments, both of the incoming 20 GeV pion and of secondary particles are identified and highlighted in the image. The track multiplicity is influenced by the shower topology and especially by the number and nature of the secondaries created. The average track multiplicity is shown as a function of the beam energy for data and various simulations in figure 7. One can

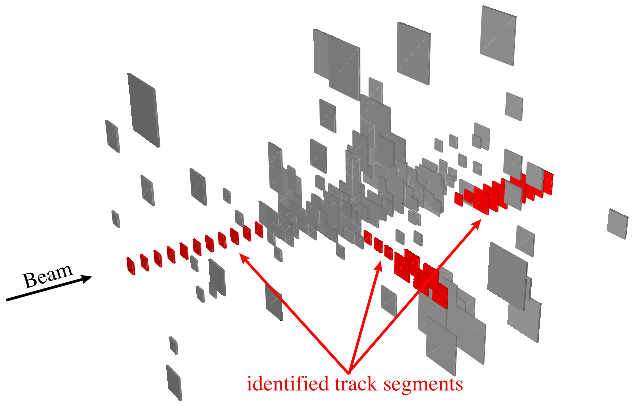

Figure 6: Event display of a pion shower in the AHCAL. In red the tiles identified by a track finding algorithm as minimum ionising segments in the particle energy deposition. Only calorimeter cells with an energy deposition higher than 0.5 MIPs are shown.

clearly see that LHEP predicts far too low average track multiplicity at all energies. The physics list closest to data in this figure is QGSP_BERT.
The energy deposited in tracks found with this algorithm is corrected for angle dependence and has also been successfully used in calibration studies. The study on the track segments is discussed in detail in ref. [36].

8.3 Longitudinal shower profiles

Thanks to the very high granularity of the CALICE calorimeters the longitudinal profile of hadronic showers can be investigated with an unprecedented accuracy. In particular, the intrinsic longitudinal development can be deconvolved from the distribution of the shower starting points. When measured with respect to the position of the first hadronic interaction, as opposed to the calorimeter front layer, hadronic showers are shorter and any layer-to-layer fluctuations introduced by calibration and dead channel effects are washed away.
The breakdown of the energy contribution from various particles in the shower ($e^{\pm}$,p, $\pi^{\pm}$, $\mu^{\pm}$) can be determined in the case of the simulated events, and is shown below. This additional information helps to understand which physics processes contribute most in which phase of the shower development. Protons and mesons are responsible for the majority of the energy deposited in the first 2-3 layers after the initial hadronic interaction at low energies (e.g. 8 GeV), while electrons and positrons take over in the layers around the shower

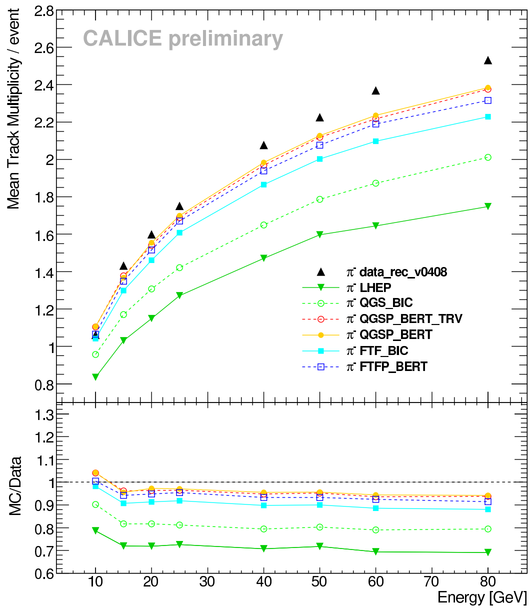

Figure 7: Average track multiplicities as a function of the beam energy for data and several physics lists.

maximum. The tail shows an almost equal contribution from hadronic and electromagnetic energy deposition.
As an example, pion events collected at three different energies have been chosen to compare the longitudinal shower profile measured in data to that obtained from MC. The various MC models playing a role at low, medium and high energies are investigated.
Figure 8 shows the longitudinal shower profiles for pions of 8, 18 and 80 GeV. The black points are data which are compared to the various MC models shown as shaded histograms. The error bars show only the systematic errors associated with the uncertainty in the determination of the first hard interaction and were estimated from comparison to profiles relative to the true first interaction layer in MC. The dominant systematic uncertainty from calibration is a 2% error on the energy scale. This would result in a coherent scaling of the whole spectrum and is therefore not shown here.
The position of the shower maximum is in general quite well simulated. All models except CHIPS tend to underestimate the tails of the showers seen in data. The longer showers in CHIPS can be expected, as discussed in section **??**. The energy dependence of the mean value (or center of gravity) and of the r.m.s. of the longitudinal shower profiles are given in figures 9 and 10, respectively. The values are taken from distributions similar to those presented

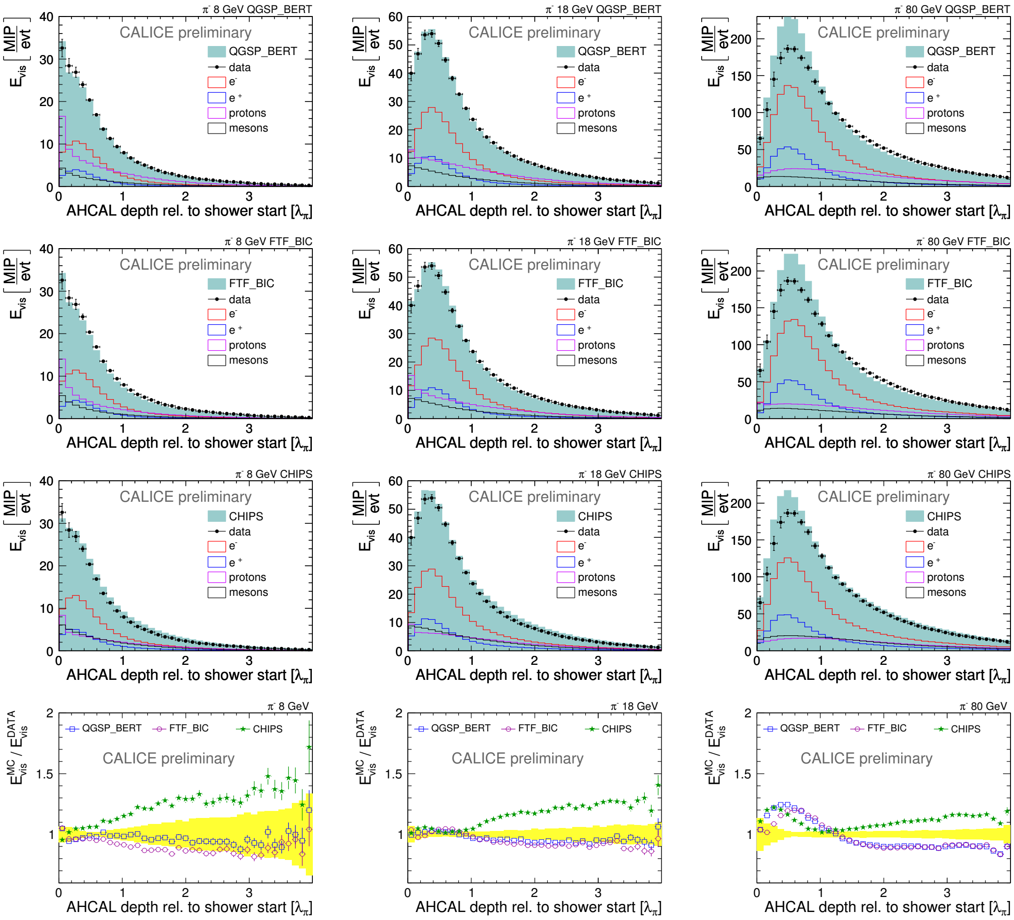

Figure 8: Longitudinal shower profile for 8, 18 and 80 GeV pions. The error bars include the statistical uncertainty and the uncertainty introduced by the determination of the first hard interaction. The breakdown of the energy contribution from various particles in the shower ($e^{\pm}$,p, $\pi^{\pm}$, $\mu^{\pm}$) is shown. The bottom raw of plots shows the ratio of simulation and data.

in figure 8 for each beam energy in the range 8–80 GeV and for the various physics lists under study. The lower right plot in both figures shows the ratio of simulation to data. At all energies the showers simulated with CHIPS predict a longer shower with a broader spread in the longitudinal direction than data. All other physics lists predict a shorter shower with a smaller longitudinal spread than data by about 3-5%. Below 25 GeV the LEP parametrisation is used in the QGSP_BERT list and this seems to match data better than the FTFP model used in QGSP_FTFP_BERT. Almost no difference is observed

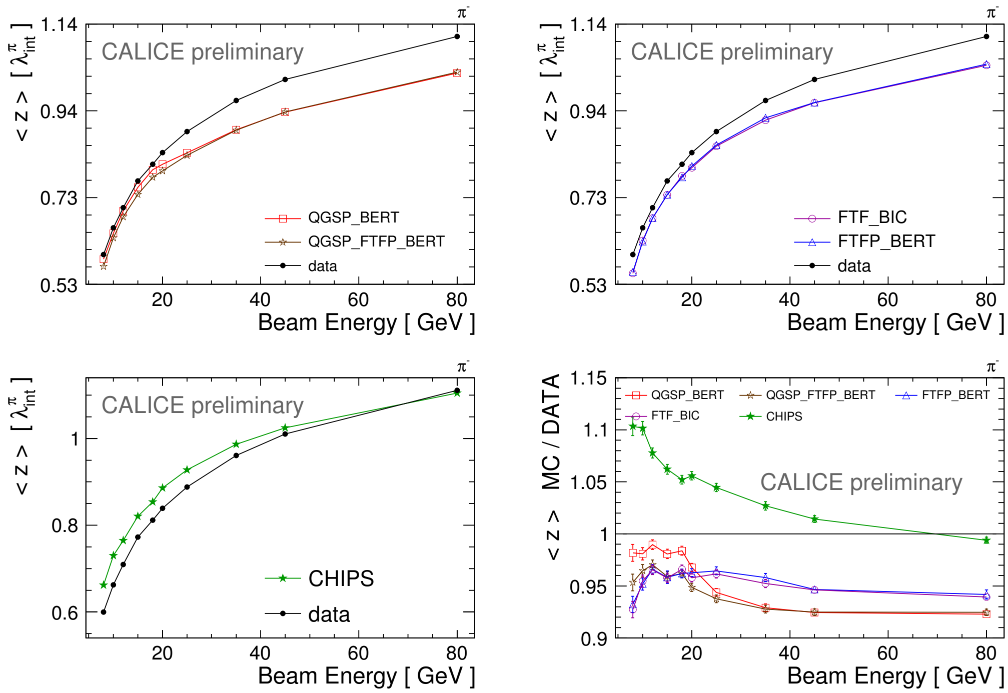

Figure 9: The mean of the longitudinal shower profile, or center of gravity in the longitudinal direction, in AHCAL data compared to various physics lists. The lower right plot shows the ratio of simulation to data.

for this variable in the combination of the FTF model with either one of the cascade models, BIC or Bertini.

8.4 Radial shower profiles

Good modeling of the transverse shower width is of importance for the development of particle flow algorithms, since it affects the degree of overlap between showers, and therefore the efficiency for separating them. For each hit in the AHCAL, we determine the transverse distance between the centre of a calorimeter cell and the projection on the calorimeter front face of the incoming particle track as determined by the tracking system. The radius of each hit is then defined as $r_i^2 = (x_i - x_{track})^2 + (y_i - y_{track})^2$, where (x_i, y_i) are the coordinates of the tile hit. By histogramming this radial distance, we form the transverse shower profile. We weight the hits by their energy, to emphasise the flow of energy in the shower. Comparisons between data and simulation are shown in figure 11 for the selected sub-sample of three energies and three

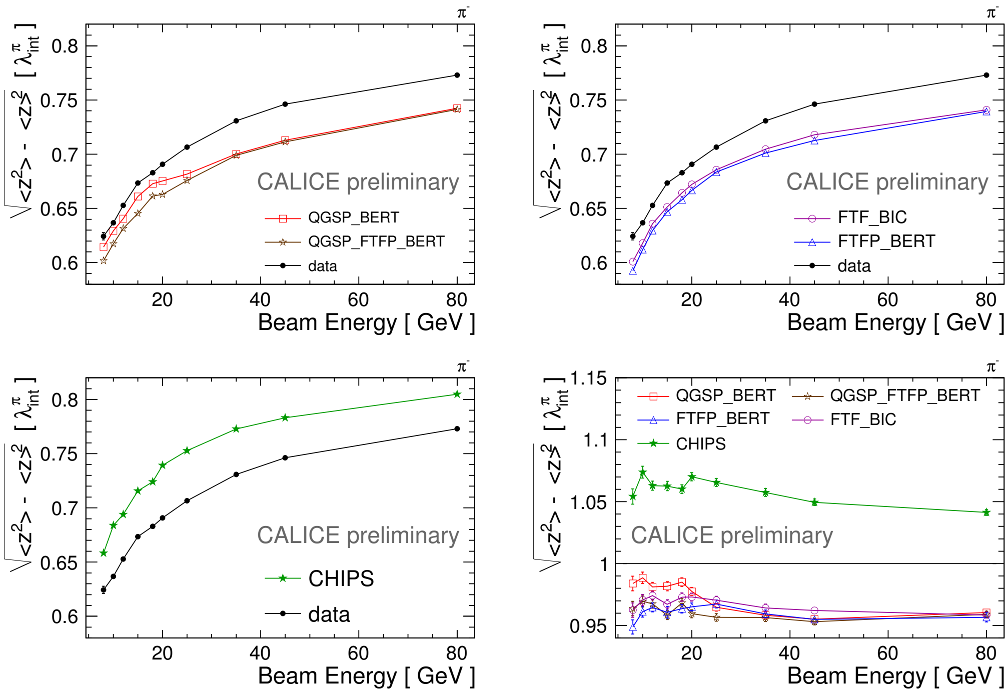

Figure 10: The r.m.s. of the longitudinal shower profile in AHCAL data compared to various physics lists. The lower right plot shows the ratio of simulation to data.

physics lists.

In order conveniently to compare all models and energies, in figure 12 we show the mean energy-weighted shower radius as a function of energy. This is the first moment of the radial energy distribution, or $\langle R\rangle = \frac{\Sigma E_i r_i}{\Sigma E_i}$. The observed shower becomes narrower with increasing energy, both in data and in all of the models. The lower right plot shows the ratio of simulation to data. All of the physics lists underestimate the shower width at all energies, typically by around 10%. The CHIPS model is closest to data for energies above 20 GeV, where it differs only by 5%.

Of course, the mean shower radius provides only one measure of the transverse shower profile. In figure 13 we show the standard deviation (RMS) of the radial energy distribution defined as RMS=$\sqrt{\langle R^2\rangle + \langle R\rangle^2}$, where $\langle R^2\rangle = \frac{\Sigma E_i r_i^2}{\Sigma E_i}$. Also in this case all physics lists underestimate the data, predicting too compact a radial shower extension. The FTF_BIC model is the closest to data at low energies (below 15 GeV) while the CHIPS model is the closest at high energies (above 15 GeV).

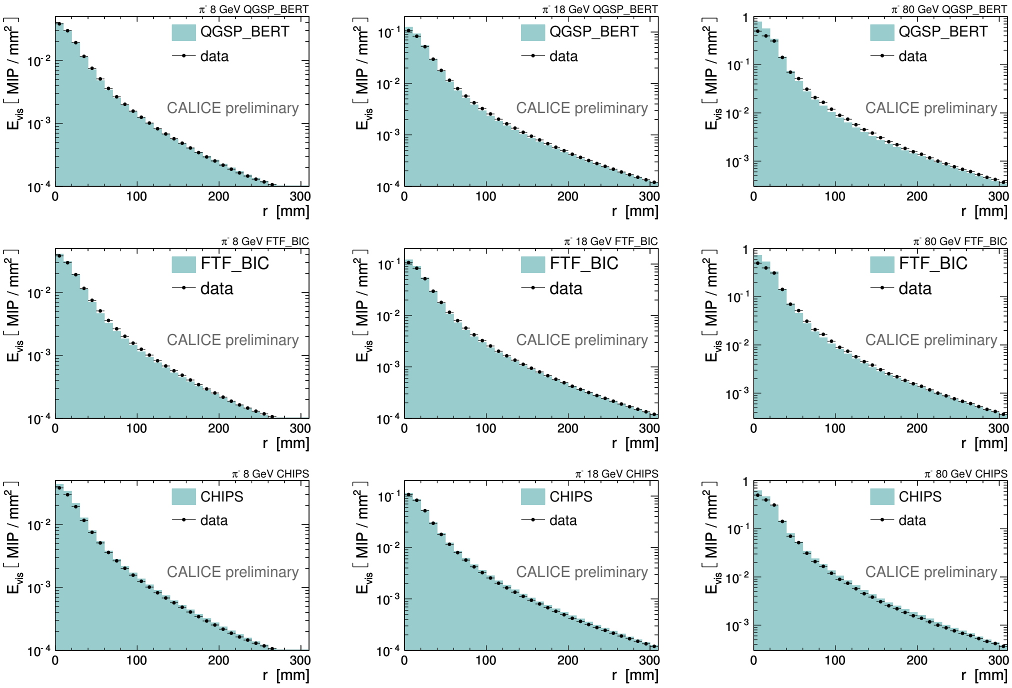

Figure 11: Radial shower profile for 8, 18 and 80 GeV pions showers in the AHCAL. Data are compared to simulation with various physics lists.

9 Validation of models using ECAL data

The event selection cuts in the ECAL analysis were designed to retain pion events wherever they interacted in the calorimeter system. A significant fraction of pions should not start to shower in the ECAL. These events are characterised by a MIP-like energy in all layers (apart from occasional δ-ray emission) and accordingly the ECAL energy shows a large peak at 50 MIPs. The fraction of such events can be used to test the interaction cross-sections in GEANT4. Most of the models give a good description of the fraction of non-interacting pions at all energies, agreeing with data within 1–2%. The LHEP physics list is the most discrepant. This gives confidence in the cross-sections simulated in GEANT4. It could also be interpreted as an indication that any residual beam contamination by kaons or (anti-)protons is small, since these species would be expected to have different interaction cross-sections.

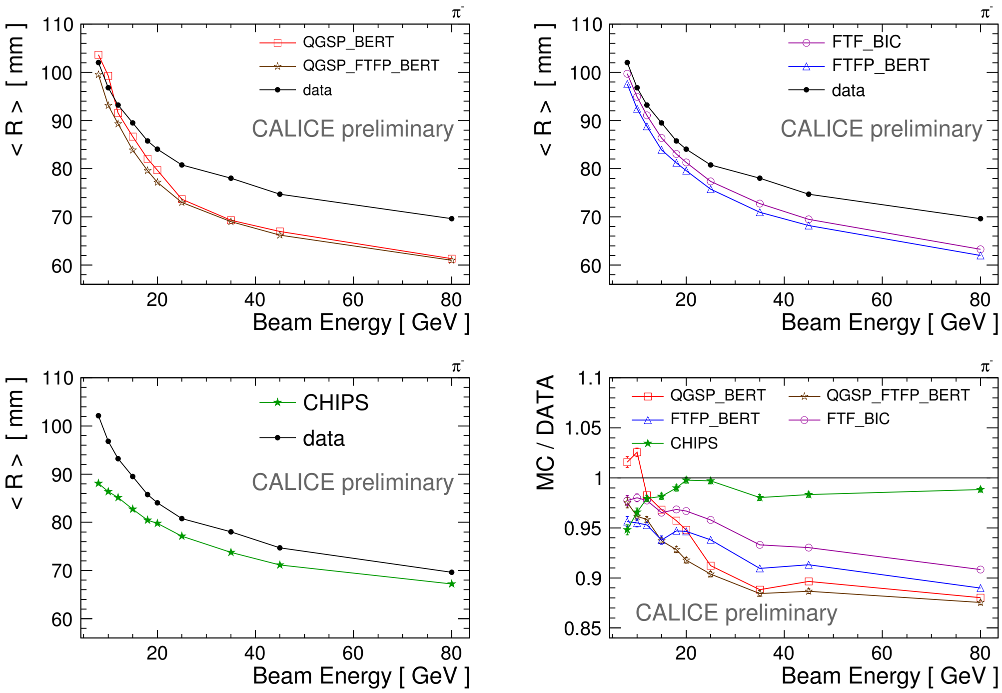

Figure 12: The first moment of the radial shower profile in AHCAL data compared to various physics lists. The lower right plot shows the ratio of simulation and data.

9.1 Total visible energy

We now consider the energy deposited in the ECAL by those pions which have their first interaction in the ECAL excluding the non-interacting ones. The mean values of the energy deposited in the ECAL is calculated for data and for all the GEANT4 physics lists under consideration, and is plotted in figure 14 in the form of ratios of simulation to data. It should be kept in mind that at best the visible energy in the ECAL is proportional to the energy deposited in $1\lambda_i$ of material, therefore not directly comparable to the value reported in figure 5.

At 8 GeV, all of the models lie within 10% of the data, and most within 5%. Both models QGSP_FTFP_BERT and FTFP_BERT show no significant energy dependence in the ratio to data. At high energies, all of the models lie 5–10% above the data. Overall, FTF_BIC is the most consistent with this aspect of the experimental data, with a maximum discrepancy of 5% at high energy.

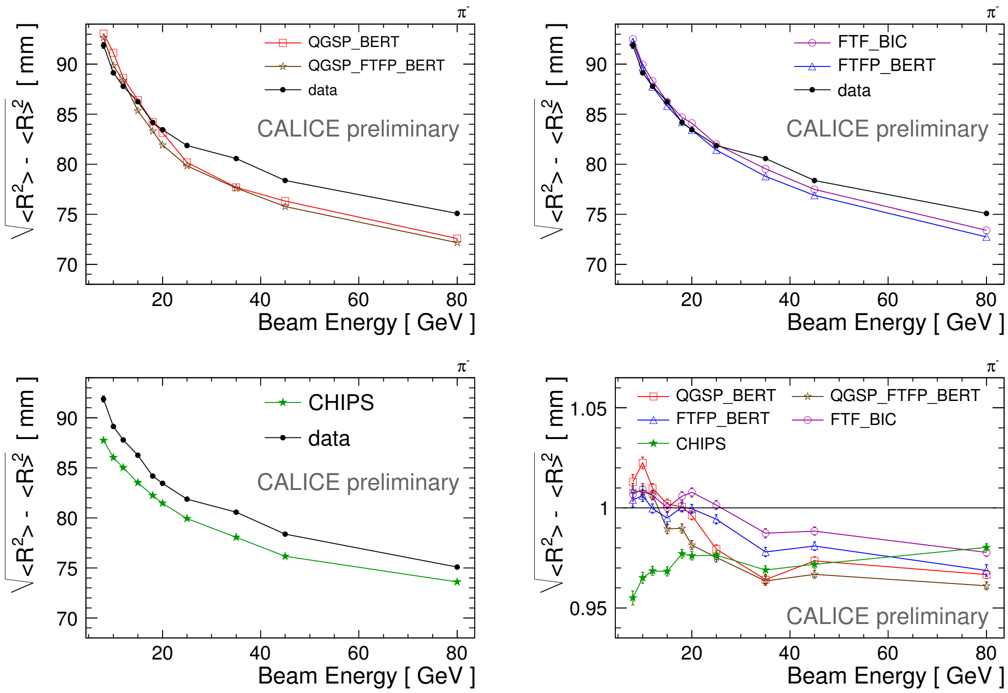

Figure 13: The second moment of the radial shower profile in AHCAL data compared to various physics lists. The lower right plot shows the ratio of simulation and data.

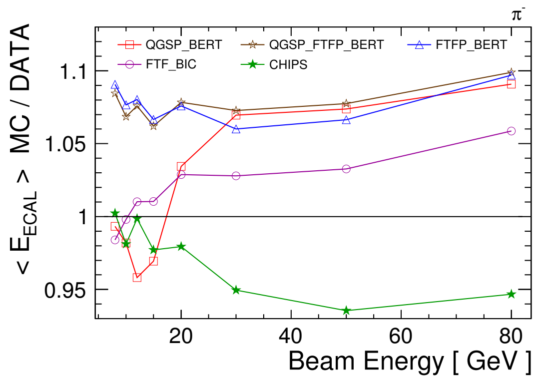

Figure 14: Ratio of simulation to data for the mean energy recorded in the ECAL, plotted as a function of beam energy. The data are compared with the predictions of simulations using different physics lists.

9.2 Longitudinal shower profiles

Even though the ECAL is not deep enough to confine hadronic showers, we were able to demonstrate in [30] that the study of the longitudinal shower profile is interesting. The combination of fine longitudinal sampling and a large ratio λ_{int}/X_0 means that the discrimination between nuclear breakup products and the electromagnetic and MIP-like hadronic components of the shower is clearer than in the iron-scintillator of the AHCAL. The first few layers after the primary interaction showed a marked peak in the data at the lower energies ($\sim 8-15$ GeV), which was ascribed to nuclear spallation products, and was not well modelled by any of the physics lists. The FTF-based models tended to overestimate this component, while the other models underestimated it. The next part of the longitudinal profile was dominated by the electromagnetic component, and was best modelled by the FTF-based models. The tails of the showers in the ECAL, dominated by mesons and energetic baryons, were reasonably modelled by all physics lists. The CHIPS model was not included in that study.

For comparison with the AHCAL results, we show in figure 15 and figure 16 respectively the mean depth (in units of λ_{int}) of the energy deposited in the ECAL and the r.m.s. of the depth about the mean. The CHIPS model is the least successful in reproducing the mean depth, while the FTF-based physics lists reproduce the data well. Likewise for the r.m.s. spread the FTF_BIC and FTF_BERT models are clearly favoured. These observations reinforce what was seen in ref. [30].

9.3 Radial shower profiles

In the ECAL case the radial shower profile is calculated with respect to the shower barycentre $(x_{\text{cog}}, y_{\text{cog}})$, i.e. $r_i^2 = (x_i - x_{\text{cog}})^2 + (y_i - y_{\text{cog}})^2$, where (x_i, y_i) are the coordinates of the ECAL silicon pad hit. Otherwise, the same procedure as for the AHCAL is used to present the mean and the r.m.s. of the radial energy distribution. shows the first moment of the radial energy distribution as a function of energy. The same behaviour as observed for the mean radius of the shower in the AHCAL as a function of energy is confirmed in figure 17 for the ECAL. The FTF models (using either BIC or Bertini cascade) lie significantly closer to the data than the QGS-based models, especially at energies above 10–15 GeV. The CHIPS model seems to reproduce the data very well for energies above 10 GeV, and is only 3% lower than data for energies below this value. In figure 18 the r.m.s. of the radial energy distribution is presented which gives a very similar message as in the case of the first moment. Also for this variable the CHIPS model seems to agree best with data.

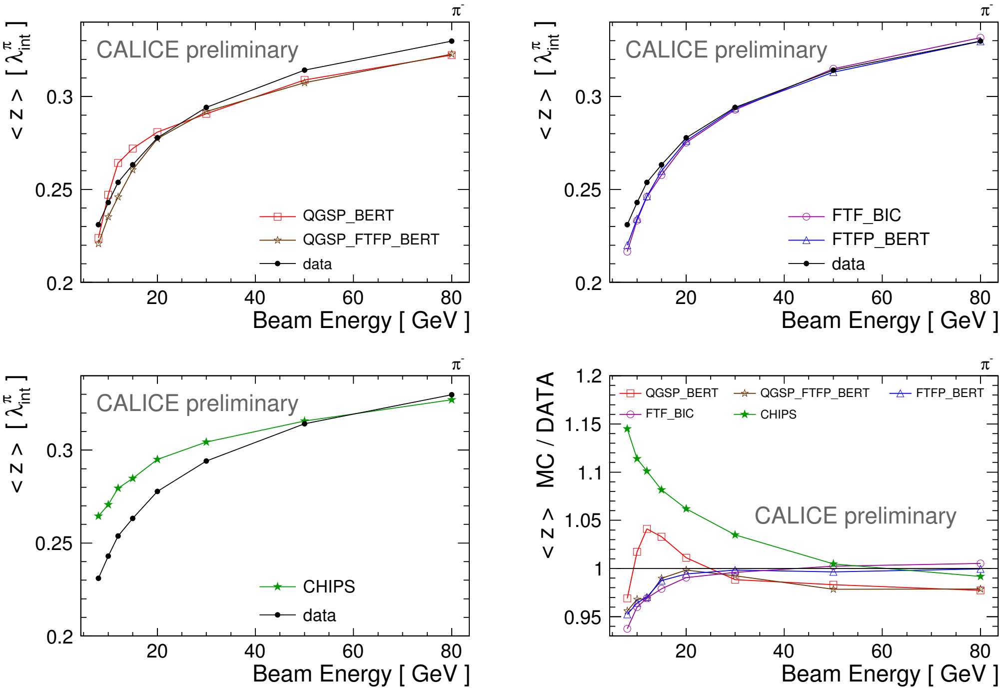

Figure 15: The first moment of the longitudinal shower profile in ECAL data compared to various physics lists. The lower right plot shows the ratio of simulation and data.

10 Improvements in Geant4

All analysis presented so far have been compared to the latest version of Geant4 9.3. In this session we briefly show the considerable improvements achieved in this last release compared to the previous one, namely Geant4 9.2. Some of these improvements were made thanks to the support of the EUDET program. Figure 19 shows the visible energy in the ECAL as presented already in figure 14 but now including the comparison to Geant4 9.2 in addition to Geant4 9.3. While there is a clear improvement of the FTF_BIC physics list the FTFP_BERT list disagrees more with the data in the newest release. The QGSP_BERT physics list remains unchanged, and QGSP_FTFP_BERT is sensitive to the improvements in FTF in the region up to 25 GeV where this model is applied.
Figure 20 is the same comparative study using the first moment of the radial shower profile in ECAL as observable.
The QGSP_BERT physics lists remained essentially unchanged, while the FTF models were significantly modified in the recent release. A clear improvement

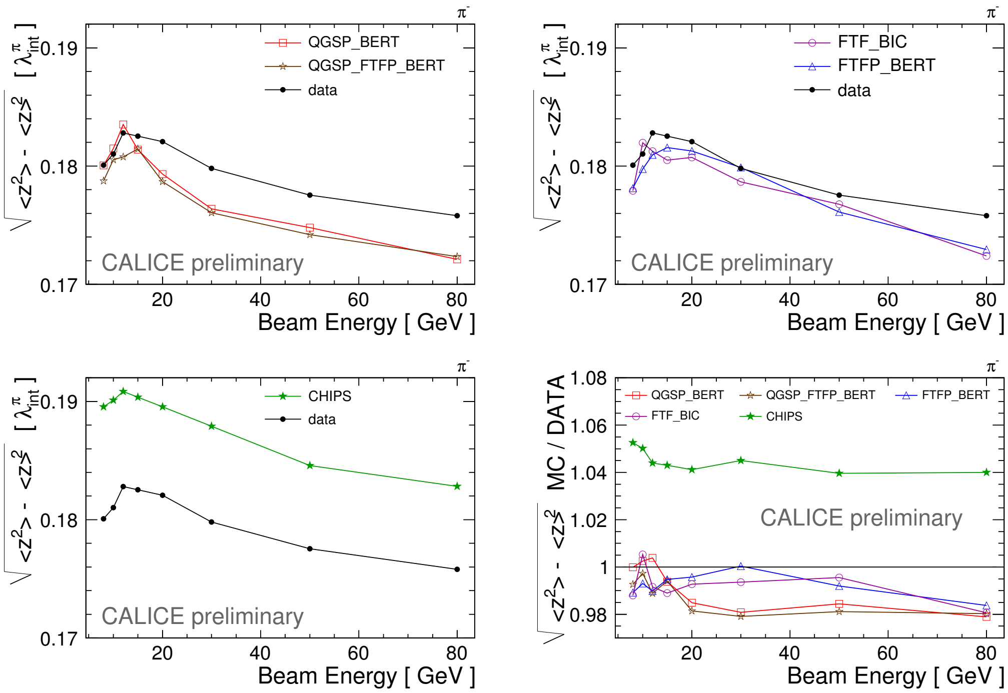

Figure 16: The second moment of the longitudinal shower profile in ECAL data compared to various physics lists. The lower right plot shows the ratio of simulation and data.

in the FTF models can be seen which brings the simulation in better agreement with data when using version 9.3.

11 Conclusion

The CALICE collaboration has built finely granular electromagnetic and hadronic calorimeters which allow in-depth studies of hadronic shower properties and validation of Monte Carlo models on an unprecedented level. With these imaging calorimeters it is possible to measure the track multiplicity, to investigate shower profiles and to determine the position of the first hard interaction in a hadronic shower.
The LHEP physics list has been omitted from most of these comparisons as it performs worse in many aspects of shower simulation. Summarizing the comparison of data with the physics lists investigated one can conclude that:

- The best agreement at the level of ∼5% is found for most of the selected observables in both ECAL and AHCAL data with the FTF-based physics

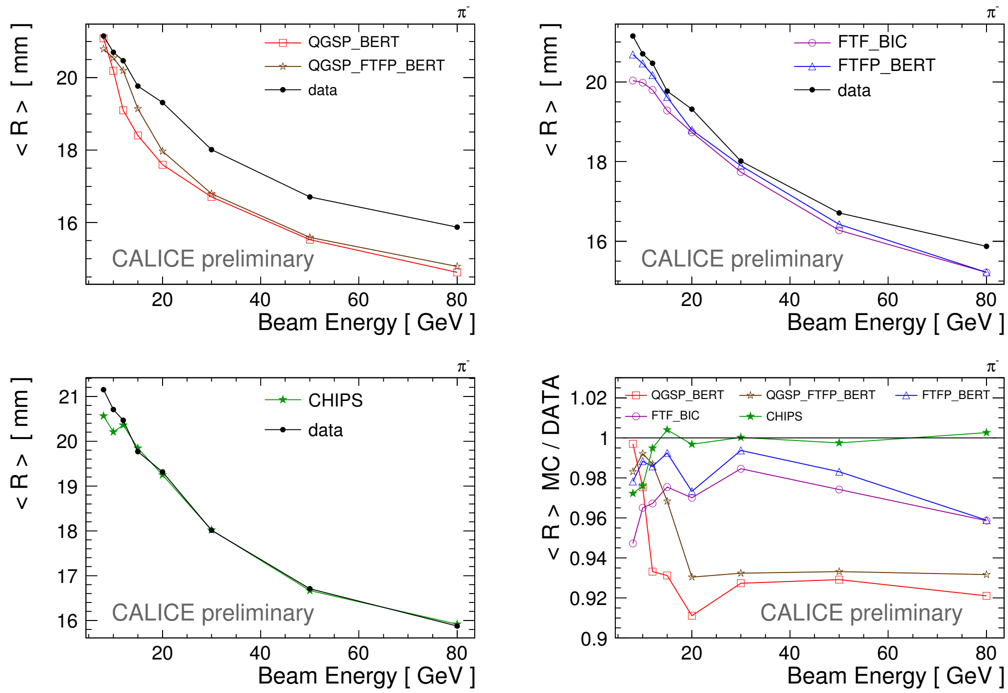

Figure 17: The mean shower radius in ECAL data compared to various physics lists. The lower right plot shows the ratio of simulation and data.

lists. The prediction for the longitudinal shower extension is only slightly narrower shower than data by less then 5%. It is still too early to draw conclusions on which of the cascade models (BIC or Bertini) best fits our data. The low energy data collected with the CALICE prototypes at FNAL are being analysed currently, and can be expected to help to further investigate the relevant energy region for this comparison.

- QGS-based lists are performing worse than FTF-based ones on the whole energy range covered. In particular the QGSP_FTFP_BERT physics list shows no clear improvement over the combination which still includes LEP as a stop-gap between QGSP and BERT.
- The CHIPS model is an experimental list still in a testing phase, but it is clearly an interesting model for CALICE. It features a smoother energy dependence and less artifacts related to the transition between different models. At present, CHIPS overestimates the visible energy in the AHCAL and the length of the shower by about 10%. In the description of the radial extension of the hadronic shower, the CHIPS model is closest to data in terms of mean shower radius, but tends to

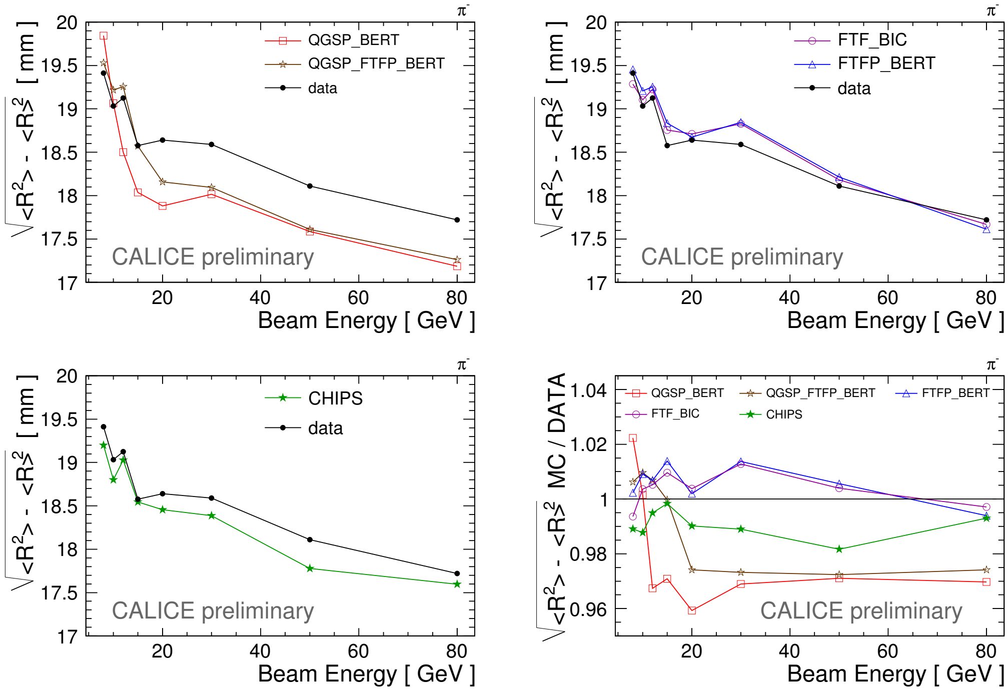

Figure 18: The r.m.s. of the radial shower profile in ECAL data compared to various physics lists. The lower right plot shows the ratio of simulation and data.

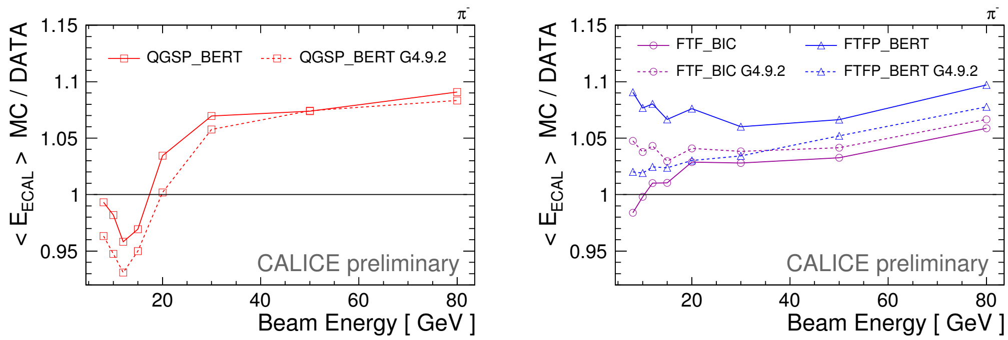

Figure 19: Comparison of Geant4 version 9.3 (solid lines) and version 9.2 (dashed lines) for the total visible energy in ECAL as a function of beam energy, on the left for the QGS-based physics lists and on the right for the FTF-based physics lists.

have a too small spread (RMS).

The CALICE collaboration acknowledge the significant improvements in the

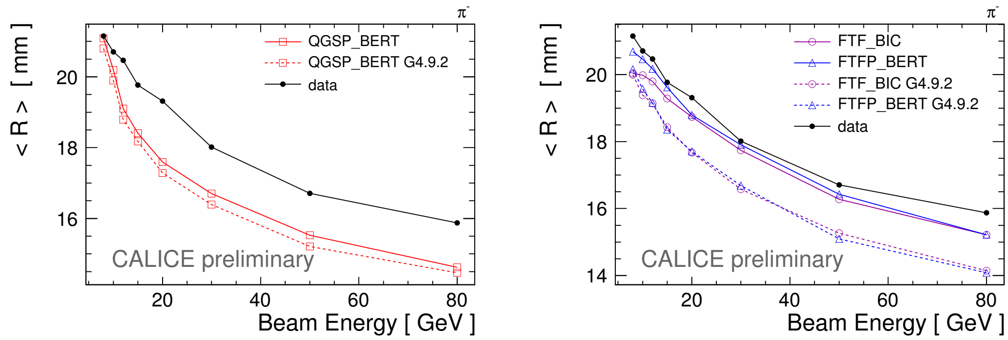

Figure 20: Comparison of Geant4 version 9.3 (solid lines) and version 9.2 (dashed lines) for the first moment of the radial shower profile in ECAL as a function of beam energy, on the left for the QGS-based physics lists and on the right for the FTF-based physics lists.

FTF model in the latest GEANT4 release. These improvements were partially made possible thanks to the EUDET project.

References

[1] N. S. Amelin, E. F. Staubo, and L. P. Csernai. Semihard collisions in Monte Carlo quark-gluon string model. *Physical Review D*, 46:4873–4881, December 1992.

[2] H.S. Fesefeldt. Simulation of hadronic showers, physics and applications. PITHA 85-02, Physikalisches Institut, RWTH Aachen, Physikalisches Institut, RWTH Aachen Physikzentrum, 5100 Aachen, Germany, September 1985.

[3] A.Heikkinen, N.Stepanov, and H.P.Wellisch. Bertini intra-nuclear cascade implementation in geant4. In *Proceedings of 2003 Conference for Computing in High- Energy and Nuclear Physics (CHEP 03), La Jolla, California*, page MOMT0086, 2003.

[4] Jose Manuel Quesada, Vladimir Ivanchenko, Anton Ivanchenko, Miguel Antonio Cortes-Giraldo, Gunter Folger, Alex Howard, and Dennis Wright. Recent developments in pre-equilibrium and de-excitation models in geant4,. In *Proceedings of the Joint International Conference on Supercomputing in Nuclear Applications and Monte Carlo 2010 (SNA + MC2010)*, 2010.

[5] B. Andersson, G. Gustafson, and B. Nilsson-Almqvist. A model for low-pt hadronic reactions with generalizations to hadron-nucleus and nucleus-nucleus collisions. *Nuclear Physics B*, 281(1-2):289 – 309, 1987.

[6] Bo Nilsson-Almqvist and Evert Stenlund. Interactions between hadrons and nuclei: The lund monte carlo - fritiof version 1.6 -. *Computer Physics Communications*, 43(3):387 – 397, 1987.

[7] Torbjorn Sjostrand. The lund monte carlo for jet fragmentation and e+e- physics - jetset version 6.2. *Computer Physics Communications*, 39(3):347 – 407, 1986.

[8] Torbjorn Sjostrand and Mats Bengtsson. The lund monte carlo for jet fragmentation and e+ e- physics - jetset version 6.3 - an update. *Computer Physics Communications*, 43(3):367–379, 1987.

[9] E Bracci, Jean Pierre Droulez, Vincenzo Flaminio, Jorn Dines Hansen, and Douglas Robert Ogston Morrison. *Compilation of cross-sections*. CERN, Geneva, 1973. Updated version of CERN-HERA 70-02 and 70-03.

[10] "S. A. Bass, M. Belkacem, M. Bleicher, M. Brandstetter, L. Bravina, C. Ernst, L. Gerland, M. Hofmann, S. Hofmann, J. Konopka, G. Mao, L. Neise, S. Soff, C. Spieles, H. Weber, L. A. Winckelmann, H. Stöcker, W. Greiner, Ch. Hartnack, J. Aichelin, and N. Amelin". Microscopic models for ultrarelativistic heavy ion collisions. *Progress in Particle and Nuclear Physics*, 41:255 – 369, 1998.

[11] M Bleicher, E Zabrodin, C Spieles, S A Bass, C Ernst, S Soff, L Bravina, M Belkacem, H Weber, and H Stacker W Greiner. Relativistic hadron-hadron collisions in the ultra-relativistic quantum molecular dynamics model. *Journal of Physics G: Nuclear and Particle Physics*, 25(9):1859, 1999.

[12] K. Abdel-Waged and V. V. Uzhinsky. Model of nuclear disintegration in high-energy nucleus nucleus interactions. *Phys. Atom. Nucl.*, 60:828–840, 1997.

[13] EMU-01 Collaboration. Complex analysis of gold interactions with photoemulsion nuclei at 10.7 gev/nucleon within the framework of cascade and fritiof models. *Zeitschrift für Physik A Hadrons and Nuclei*, 358:337–351, 1997. 10.1007/s002180050337.

[14] Kh Abdel-Waged and V V Uzhinskii. Estimation of nuclear destruction using aladin experimental data. *Journal of Physics G: Nuclear and Particle Physics*, 24(9):1723, 1998.

[15] I. A. Pshenichnov, J. P. Bondorf, I. N. Mishustin, A. Ventura, and S. Masetti. Mutual heavy ion dissociation in peripheral collisions at ultrarelativistic energies. *Phys. Rev. C*, 64(2):024903, Jul 2001.

[16] A. Bolshakova, I. Boyko, G. Chelkov, D. Dedovitch, A. Elagin, M. Gostkin, S. Grishin, A. Guskov, Z. Kroumchtein, Yu. Nefedov, K. Nikolaev, A. Zhemchugov, F. Dydak, J. Wotschack, A. De Min, V. Ammosov, V. Gapienko, V. Koreshev, A. Semak, Yu. Sviridov, E. Usenko, and V. Zaets. Cross-sections of large-angle hadron production in proton– and pion–nucleus interactions ii: beryllium nuclei and beam momenta from ±3 gev/c to ±15 gev/c;. *The European Physical Journal C - Particles and Fields*, 62:697–754, 2009. 10.1140/epjc/s10052-009-1092-1.

[17] A. Bolshakova, I. Boyko, G. Chelkov, D. Dedovitch, A. Elagin, M. Gostkin, A. Guskov, Z. Kroumchtein, Y. Nefedov, K. Nikolaev, A. Zhemchugov, F. Dydak, J. Wotschack, A. De Min, V. Ammosov, V. Gapienko, V. Koreshev, A. Semak, Y. Sviridov, E. Usenko, and V. Zaets. Cross sections of large-angle hadron production in proton– and pion–nucleus interactions iii: tantalum nuclei and beam momenta from ±3 gev/c to ±15 gev/c;. *The European Physical Journal C - Particles and Fields*, 63:549–609, 2009. 10.1140/epjc/s10052-009-1114-z.

[18] A. Bolshakova, I. Boyko, G. Chelkov, D. Dedovitch, A. Elagin, M. Gostkin, A. Guskov, Z. Kroumchtein, Yu. Nefedov, K. Nikolaev, A. Zhemchugov, F. Dydak, J. Wotschack, A. De Min, V. Ammosov, V. Gapienko, V. Koreshev, A. Semak, Yu. Sviridov, E. Usenko, and V. Zaets. Cross-sections of large-angle hadron production in proton– and pion–nucleus interactions iv: copper nuclei and beam momenta from ±3 gev/c to ±15 gev/c;. *The European Physical Journal C - Particles and Fields*, 64:181–241, 2009. 10.1140/epjc/s10052-009-1144-6.

[19] A. De Roeck, F. Gianotti, A. Morsch, and W. Pokorski. Simulation physics requirements from the lhc experiments. Technical report, CERN, 2004.

[20] C. Alexa, J. Apostolakis, S. Banerjee, S. Constantinescu, A. De Roeck, S. Dita, A. Dotti, D. Elvira, F. Gianotti, A. Kiryunin, A. Lupi, C. Roda, i D. Salihagic, P. Schacht, P. Strizenec, and H.-P. Wellisch. Geant4 hadronic physics validation with lhc test-beam data: first conclusions. Technical report, CERN, 2004.

[21] A. Ribon, J. Apostolakis, A. Dotti, G. Folger, V. Ivanchenko, M. Kosov, V. Uzhinsky, and D. H. Wright. Status of geant4 hadronic physics for the simulation of lhc experiments at the lhc physics program. Technical report, CERN, 2010.

[22] TileCal Collaboration. Testbeam studies of production modules of the atlas tile calorimeter. *Nuclear Instruments and Methods in Physics Research A*, 606:362 – 394, 2009.

[23] TileCal Collaboration. Study of the response of the atlas central calorimeter to pions of energies from 3 to 9 gev. *Nuclear Instruments and Methods in Physics Research A*, 607:372 – 386, 2009.

[24] "P. Adragna, C. Alexa, K. Anderson, A. Antonaki, A. Arabidze, L. Batkova, V. Batusov, H.P. Beck, E. Bergeaas Kuutmann, C. Biscarat, G. Blanchot, A. Bogush, C. Bohm, V. Boldea, M. Bosman, C. Bromberg, J. Budagov, D. Burckhart-Chromek, M. Caprini, L. Caloba, D. Calvet, T. Carli, J. Carvalho, M. Cascella, J. Castelo, M.V. Castillo, M. Cavalli-Sforza, V. Cavasinni, A.S. Cerqueira, C. Clement, M. Cobal, F. Cogswell, S. Constantinescu, D. Costanzo, A. Corso-Radu, C. Cuenca, D.O. Damazio, T. Davidek, K. De, T. Del Prete, B. Di Girolamo, S. Dita, T. Djobava, M. Dobson, A. Dotti, R. Downing, I. Efthymiopoulos, D. Eriksson, D. Errede, S. Errede, A. Farbin, D. Fassouliotis, R. Febbraro, A. Fenyuk, C. Ferdi, A. Ferrer, V. Flaminio, D. Francis, E. Fullana, S. Gadomski, S. Gameiro, V. Garde, K. Gellerstedt, V. Giakoumopoulou, O. Gildemeister, V. Gilewsky, N. Giokaris, N. Gollub, A. Gomes, V. Gonzalez, B. Gorini, P. Grenier, P. Gris, M. Gruwe, V. Guarino, C. Guicheney, A. Gupta, C. Haeberli, H. Hakobyan, M. Haney, S. Hellman, A. Henriques, E. Higon, S. Holmgren, M. Hurwitz, J. Huston, C. Iglesias, A. Isaev, I. Jen-La Plante, K. Jon-And, M. Joos, T. Junk, A. Karyukhin, A. Kazarov, H. Khandanyan, J. Khramov, J. Khubua, S. Kolos, I. Korolkov, P. Krivkova, Y. Kulchitsky, Yu. Kurochkin, P. Kuzhir, T. Le Compte, R. Lefevre, G. Lehmann, R. Leitner, M. Lembesi, J. Lesser, J. Li, M. Liablin, M. Lokajicek, Y. Lomakin, A. Lupi, C. Maidanchik, A. Maio, M. Makouski, S. Maliukov, A. Manousakis, L. Mapelli, C. Marques, F. Marroquim, F. Martin, E. Mazzoni, F. Merritt, A. Miagkov, R. Miller, I. Minashvili, L. Miralles, G. Montarou, M. Mosidze, A. Myagkov, S. Nemecek, M. Nessi, L. Nodulman, B. Nordkvist, O. Norniella, J. Novakova, A. Onofre, M. Oreglia, D. Pallin, D. Pantea, J. Petersen, J. Pilcher, J. Pina, J. Pinhão, F. Podlyski, X. Portell, J. Poveda, L. Pribyl, L.E. Price, J. Proudfoot, M. Ramstedt, R. Richards, C. Roda, V. Romanov, P. Rosnet, P. Roy, A. Ruiz, V. Rumiantsev, N. Russakovich, O. Saltó,

B. Salvachua, E. Sanchis, H. Sanders, C. Santoni, J.G. Saraiva, F. Sarri, I. Satsunkevitch, L.-P. Says, G. Schlager, J. Schlereth, J.M. Seixas, B. Selldèn, N. Shalanda, P. Shevtsov, M. Shochet, J. Silva, P. Da Silva, V. Simaitis, M. Simonyan, A. Sissakian, J. Sjölin, C. Solans, A. Solodkov, I. Soloviev, O. Solovyanov, M. Sosebee, F. Spanò, R. Stanek, E. Starchenko, P. Starovoitov, P. Stavina, M. Suk, I. Sykora, F. Tang, P. Tas, R. Teuscher, S. Tokar, N. Topilin, J. Torres, L. Tremblet, P. Tsiareshka, M. Tylmad, D. Underwood, G. Unel, G. Usai, A. Valero, S. Valkar, J.A. Valls, A. Vartapetian, F. Vazeille, I. Vichou, V. Vinogradov, I. Vivarelli, M. Volpi, A. White, A. Zaitsev, A. Zenine, and T. Zenis". Measurement of pion and proton response and longitudinal shower profiles up to 20 nuclear interaction lengths with the atlas tile calorimeter. *Nuclear Instruments and Methods in Physics Research Section A: Accelerators, Spectrometers, Detectors and Associated Equipment*, 615(2):158 – 181, 2010.

[25] IEEE, editor. *Transition between hadronic models in Geant4*, 2009.

[26] *Recent improvements on the description of hadronic interactions in Geant4*, 2010.

[27] Brient, Jean-Claude and Videau, Henri. The calorimetry at the future e+ e- linear collider. In *Proceedings of APS / DPF / DPB Summer Study on the Future of Particle Physics (Snowmass 2001), Snowmass, Colorado*, July 2001.

[28] Morgunov, V. L. Calorimetry design with energy-flow concept (imaging detector for high-energy physics). In *Proceedings of the Tenth International Conference Pasadena, California, USA*, March 2002.

[29] Thomson, M. A. Particle Flow Calorimetry and the PandoraPFA Algorithm. *Nucl. Instrum. Meth.*, A611:25–40, 2009.

[30] C. Adloff, Y. Karyotakis, J. Repond, J. Yu, G. Eigen, et al. Study of the interactions of pions in the CALICE silicon-tungsten calorimeter prototype. *JINST*, 5:P05007, 2010.

[31] Adloff, C. and others. Construction and Commissioning of the CALICE Analog Hadron Calorimeter Prototype. *JINST*, 5:P05004, 2010.

[32] C. Adloff et al. Response of the CALICE Si-W Electromagnetic Calorimeter Physics Prototype to Electrons. *J. Phys. Conf. Ser.*, 160:012065, 2009.

[33] The CALICE collaboraation. Electromagnetic response of a highly granular Hadronic Calorimeter. 2010. article in preparation.

[34] Mokka Working Group. Mokka - a GEANT4 application to simulate the full ILD geometry. http://polzope.in2p3.fr:8081/MOKKA.

[35] M. Kosov. CHIPS physics list in Geant4. http://ilcagenda.linearcollider.org/getFile.py/access?contribId=126&sessionId=31&resId=0&materialId=slides&confId=4649.

[36] F. Simon, L. Weuste. Identification of track segments in hadronic showers in the analog hadron calorimeter - algorithm and comparisons to simulations. *CALICE Analysis Note*, 022, July 2010.